The Astrophysical Journal Letters, 804:L1 (5pp), 2015 May 1 doi:10.1088/2041-8205/804/1/L1

THIN CURRENT SHEETS AND ASSOCIATED ELECTRON HEATING IN TURBULENT SPACE PLASMA

A. Chasapis[1], A. Retinò[1], F. Sahraoui[1], A. Vaivads[2], Yu. V. Khotyaintsev[2],
D. Sundkvist[4], A. Greco[3], L. Sorriso-Valvo[5], and P. Canu[1]
[1] Laboratoire de Physique des Plasmas, Ecole Polytechnique, Palaiseau, F-91128, France; alexandros.chasapis@lpp.polytechnique.fr
[2] Swedish Institute of Space Physics, Uppsala, Sweden
[3] Dipartimento di Fisica, Universita della Calabria, Italy
[4] Space Sciences Laboratory, University of California, Berkeley, CA, USA
[5] IMIP-CNR, U.O.S. LICRYL di Cosenza, Italy
Received 2015 January 27; accepted 2015 February 16; published 2015 April 23

ABSTRACT

Intermittent structures, such as thin current sheets, are abundant in turbulent plasmas. Numerical simulations indicate that such current sheets are important sites of energy dissipation and particle heating occurring at kinetic scales. However, direct evidence of dissipation and associated heating within current sheets is scarce. Here, we show a new statistical study of local electron heating within proton-scale current sheets by using high-resolution spacecraft data. Current sheets are detected using the Partial Variance of Increments (PVI) method which identifies regions of strong intermittency. We find that strong electron heating occurs in high PVI (>3) current sheets while no significant heating occurs in low PVI cases (<3), indicating that the former are dominant for energy dissipation. Current sheets corresponding to very high PVI (>5) show the strongest heating and most of the time are consistent with ongoing magnetic reconnection. This suggests that reconnection is important for electron heating and dissipation at kinetic scales in turbulent plasmas.

Key words: acceleration of particles – magnetic fields – magnetic reconnection – plasmas – turbulence

1. INTRODUCTION

Turbulent plasmas are characterized by intermittent structures such as current sheets, magnetic islands, vortices, and shocklets (Bruno & Carbone 2013). At kinetic scales, in the so-called dissipation range of turbulence, such structures are responsible for substantial energy dissipation and particle heating and acceleration (Wan et al. 2012; Karimabadi et al. 2014). One important dissipation mechanism is magnetic reconnection (Vaivads et al. 2006). In turbulence, magnetic reconnection takes place in thin current sheets, as shown by numerical simulations (Matthaeus & Lamkin 1986; Servidio et al. 2009; Zank et al. 2014) and verified by spacecraft data (Retinò et al. 2007; Sundkvist et al. 2007).

Space plasmas offer a privileged environement to study current sheets and associated dissipation, in particular, the near-Earth space where high-resolution spacecraft measurements are available. Several studies have been done on the formation of current sheets in the pristine solar wind (Chian & Muñoz 2011; Miao et al. 2011; Perri et al. 2012; Zhdankin et al. 2012; Vörös et al. 2014) as well as the associated reconnection (Gosling 2007; Osman et al. 2014). The turbulent plasma of Earth's magnetosheath has been studied in simulations that showed such current sheets downstream of the quasi-parallel shock, producing local dissipation (Karimabadi et al. 2014). Magnetic reconnection has been observed in proton-scale current sheets (Retinò et al. 2007), and their role as a dissipation process at those scales has been considered (Sundkvist et al. 2007). However, a quantitative experimental estimation of particle heating in thin current sheets within turbulence has not yet been reported. Such heating is direct evidence of energy dissipation at small scales. This work presents a novel statistical study of electron heating within thin current sheets in the turbulent plasma of the Earth's magnetosheath, downstream of the quasi-parallel bow shock.

2. DATA

We use data from the *Cluster* spacecraft (Escoubet et al. 1997) and focus on one event during which the spacecraft observed the Earth's magnetosheath downstream of the quasi-parallel shock. This region is one of the most turbulent in the near-Earth space and is characterized by the formation of many different small-scale coherent structures such as current sheets, magnetic islands, and vortices (Karimabadi et al. 2014). We select a data interval of one and a half hours inside the magnetosheath during which all instruments on board *Cluster* operated in high-resolution mode (Burst Mode). The same data set was used in Retinò et al. (2007) and Sundkvist et al. (2007), however, analysis of electron data was not performed in detail. During this event, the separation of the four *Cluster* spacecraft was 100 km, which in Earth's magnetosheath is comparable to the proton inertial length $d_i = c/\omega_{pi}$, where ω_{pi} is the proton plasma frequency. This event is therefore very appropriate to study structures having scales of the order of d_i.

In this event, the flux-gate magnetometer (FGM instrument) measures the three components of the magnetic field with a sampling frequency of 67 Hz (Balogh et al. 1997). An overview of the magnetic field data measured by the FGM instrument of *Cluster*1 can be seen in Figure 1. The lower panel of this figure presents one component of the magnetic field during a shorter interval of time where the detected current sheets are highlighted.

The electron distribution functions are measured by the PEACE instrument (Johnstone et al. 1997). During this event, the PEACE instrument measureed two-dimensional slices of the full three-dimensional distribution function every $dt = 0.125$ s which corresponds to an azimuthal angle of 11°.25 in the spacecraft spin plane. Each slice is composed of 12 bins in polar angle (with respect to the spin plane) and the measurements cover 32 energy channels in the range 0.6 eV –26 keV. The full three-dimensional distribution

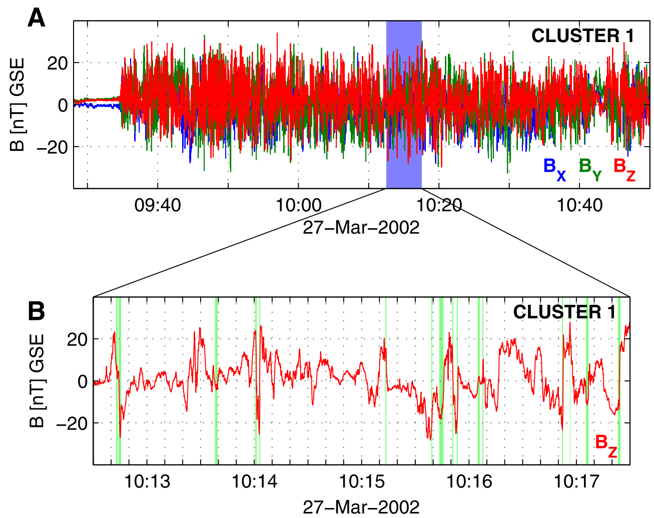

Figure 1. Interval of magnetic field data from *Cluster*1 in the GSE coordinate system. The upper panel shows the evolution of the magnetic field components during the interval used for this analysis. The four spacecraft cross the bow shock at 09:35 and enter into the magnetosheath. The lower panel shows the z-component of the magnetic field during a shorter interval. The detected current sheets are shown by green highlighted bands.

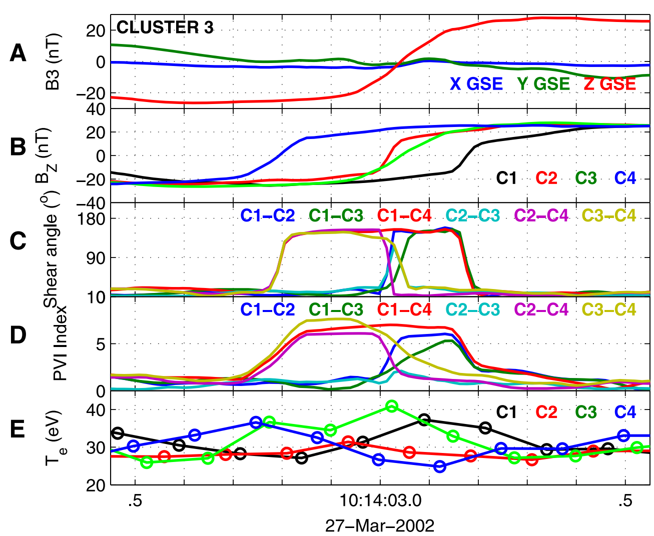

Figure 2. Example of a detected current sheet. Panel (A) shows the magnetic field measured by *Cluster*3. Panel (B) shows the z-component in GSE coordinates for the four spacecraft. Panels (C) and (D) show the measured angle of the magnetic field vectors and the PVI index for each pair of spacecraft. Panel (E) shows the estimated electron temperature for each spacecraft.

function was obtained as the spacecraft rotated around its spin axis, covering all azimuth angles during one spin of 4 s. Given the typical velocities at which current sheets move in the magnetosheath, the duration of the crossing of one thin current sheet is 0.5 s (see Figure 2). Therefore, higher time resolution than spin resolution is needed to resolve electron heating. In this study, we use such two-dimensional slices of the distribution function at sub-spin resolution $dt = 0.125$ s to study electron heating at small scales, as performed earlier by Khotyaintsev et al. (2006), Nakamura et al. (2006), Retinò et al. (2006), Retinò et al. (2007), Schwartz et al. (2011), and Varsani et al. (2014) in different regions of space. Such slices are well representative of the thermal part (core) of the full distribution in the magnetosheath, since the thermal speed of

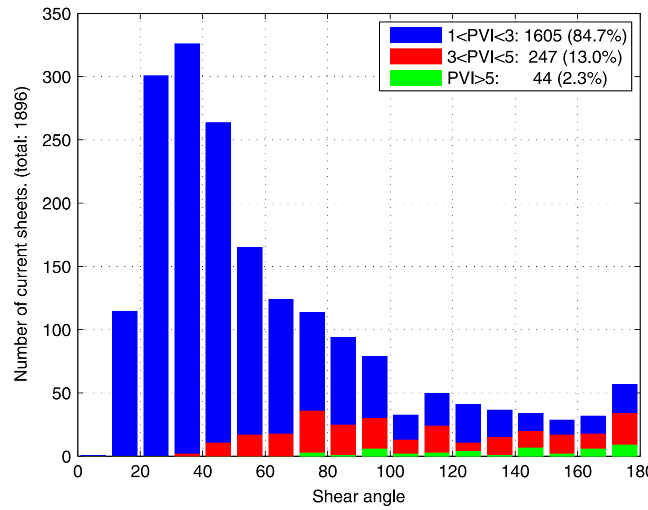

Figure 3. Distribution of the detected current sheets as a function of the magnetic shear angle. Each color represents a different value of the PVI threshold. The total number of detected current sheets is 1896.

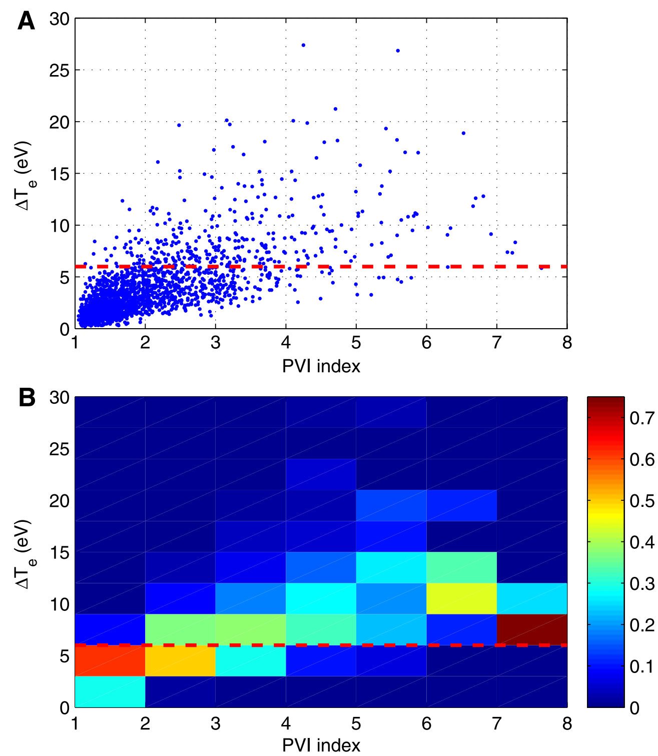

Figure 4. Local increase of the electron temperature and corresponding PVI index for each of the detected structures. Panel (A): scatter plot of the values for each detected current sheets. Panel (B): normalized histograms are shown along the y axis for each slice of PVI index values. The dashed red line in both plots denotes the $1\sigma_{T_e}$ level for the estimated electron temperature during the whole interval.

electrons is typically much larger than the bulk flow speed. Furthermore, the anisotropy of the core is typically small in the magnetosheath, as directly verified by comparing the distribution function at different polar angles. Therefore, we average over all polar angles, everywhere using omidirectional distributions. We obtain a proxy of the electron temperature from such omnidirectional distributions, as discussed in Section 4.

Table 1
Percentage Distribution of the Electron Heating for Structures with Different PVI Values

PVI	$\Delta T < 1\sigma$	$1\sigma < \Delta T < 2\sigma$	$2\sigma < \Delta T < 3\sigma$	$\Delta T > 3\sigma$	Total
Low (PVI < 3)	90.7%	8.7%	0.5%	0.1%	100.0%
High (3 < PVI < 5)	43.3%	43.7%	9.3%	3.7%	100.0%
Very High (PVI > 5)	20.4%	52.3%	18.2%	9.1%	100.0%

3. CURRENT SHEET DETECTION

The approach we used to detect current sheets was an implementation of the partial variance of increments (PVI) method (Greco et al. 2008, 2009). This method relies on the calculation of the vector $|\Delta \boldsymbol{B}_{ij}(t)| = |\boldsymbol{B}_i(t) - \boldsymbol{B}_j(t)|$, where t is the time of every measurement and where $i, j = 1, 2, 3, 4$ identify the four *Cluster* spacecraft. From that, we calculate the normalized partial variance of increments index (PVI index):

$$\mathrm{PVI}_{ij}(t) = \sqrt{\frac{\left|\Delta \boldsymbol{B}_{ij}(t)\right|^2}{\left\langle \left|\Delta \boldsymbol{B}_{ij}\right|^2 \right\rangle}}, \tag{1}$$

where $\langle|\Delta \boldsymbol{B}_{ij}|^2\rangle$ denotes the time average over the span of the time-series.

For single spacecraft data, previous studies used the PVI index computed from temporal increments of the magnetic field: $|\Delta \boldsymbol{B}_\tau(t)| = |\boldsymbol{B}(t+\tau) - \boldsymbol{B}(t)|$ (Greco et al. 2008). In the case of a multi-spacecraft mission such as *Cluster*, this can be done using the increments of the magnetic field measured simultaneously by two spacecraft separated by a distance d: $|\Delta \boldsymbol{B}_d(t)| = |\boldsymbol{B}_{r+d}(t) - \boldsymbol{B}_r(t)|$. Such an approach will provide reliable results for structures of scales comparable to the separation d of the two spacecraft (in the present study $d \sim d_i$, the proton inertial length). However, these two approaches give similar results when the value of τ is set to the proton inertial length times the average flow velocity in the magnetosheath, $\tau \sim d_i/v_f \sim d/v_f$. From Equation 1, we expect to observe a peak in the PVI index when there is a sharp variation of the magnetic field between a pair of spacecraft correspoding to a region of strong current. As PVI increases to values of 3 or more, the detected discontinuities are extremely likely to be associated with structures that form the non-Gaussian tails of the probability distribution function of the signal (Greco et al. 2008, 2009). Thus, as the threshold is increased, stronger and rarer events are identified. Such structures, characterized by a thin region of strong current, have been shown numerically to be important for particle heating and, consequently, dissipation (Osman et al. 2011). We have estimated the current (not shown) using the multi-spacecraft approach described in Dunlop et al. (2002). This allows us to verify that peaks of high PVI index indeed correspond to regions of strong current as expected. One example of the detected current sheets is shown in Figure 2(D). In this case, the peaks of the PVI index for each pair can be clearly seen as the four spacecraft cross the boundary. For this study we set the condition to $\mathrm{PVI}_{ij} > 1$ for at least one pair of spacecraft and selected only the portions of the time-series that satisfy this condition. As for high PVI current sheets, we considered the cases where $\mathrm{PVI}_{ij} > 3$. This study focuses on proton scales which, in this case, correspond to 100–200 km. Typical velocities in the magnetosheath are in the range of 50–400 km s^{-1}. In order to retain proton-scale structures, a limit was set on the duration of the structures, choosing only those which last between 0.25 and 8 s.

Previous studies focused on the rotation of the magnetic field across current sheets (Li 2008; Miao et al. 2011; Zhdankin et al. 2012). This magnetic shear angle has been approached both as an identification method as well as an important element for the physical processes of a current sheet (e.g., instabilities, magnetic reconnection onset). The magnetic shear angle is calculated by measuring the rotation of the magnetic field as the spacecraft cross the boundary. This method has been implemented for the study of current sheets in the solar wind (Chian & Muñoz 2011). In this case, the angle that was measured was between each pair of spacecraft, as was done for the PVI index:

$$\theta_{ij}(t) = \cos^{-1}\frac{\boldsymbol{B}_i(t)\cdot\boldsymbol{B}_j(t)}{\left|\boldsymbol{B}_i(t)\right|\cdot\left|\boldsymbol{B}_j(t)\right|}. \tag{2}$$

An example of a crossing of a current sheet can be seen in Figure 2. Note that for this case, the GSE frame is very close to the current sheet frame obtained from minimum variance analysis of the magnetic field. The reversal of the B_z component indicates when each spacecraft crosses the boundary. Figure 2(C) shows the shear angle between each pair of spacecraft calculated as described above. The PVI index is shown in Figure 2(D) and exhibits a peak similar to that of the shear angle, as expected since this current sheet is characterized by large rotation but small change in the overall field strength. Figure 2(A) shows a negative/positive perturbation of the out-of-plane B_y component of the magnetic field around the center of the current sheet where B_z reverses its sign. Such perturbation in the out-of-plane component corresponds to the quadrupolar Hall magnetic field expected in the diffusion region of magnetic reconnection (Sonnerup 1979; Vaivads et al. 2004; Retinò et al. 2007). Figure 2(D) shows the estimated electron temperature. The four spacecraft measure an enhancement of the electron temperature within the current sheet. The very high PVI index, the quadrupolar Hall signature in the magnetic field, and the increase in the estimated electron temperature demonstrate that this case is very likely to be a reconnection site similar to the one studied in Retinò et al. (2007).

The distribution of the detected structures with respect to their shear angle is shown in Figure 3 for different values of the PVI threshold. We observe two distinct populations. One comprises the bulk of the overall population (~85%) with low PVI (1 < PVI < 3) and mostly low shear angles. A second, smaller population was observed having a high PVI (3 < PVI < 5) index and relatively large rotation angles. In particular, very high PVI (PVI > 5) cases correspond to rotation angles larger than ~90°. On the other hand, structures with high PVI and low magnetic shear angle are scarce.

4. ELECTRON HEATING

We now study electron heating by evaluating the increase in the electron temperature within each current sheet. We compute a proxy of the electron temperature T_e at high time resolution $dt = 0.125$ s from two-dimensional slices of the distribution function $f_e(E)$ averaged over polar angles. Since the temperature in the magnetosheath is dominated by the core of the distribution function, we limit the energy range to the core ($E < 832$ eV) and exclude supra-thermal electrons. Assuming that the core of the distribution is Maxwellian, the maximum of the differential energy flux $dEF_e(E) = 2\frac{E^2}{m_e^2}f_e(E)$ is twice the temperature T_e (Lewis et al. 2008). Visual inspection of the electron distributions indicates that the core is indeed well represented by a Maxwellian and confirms the validity of the method. At low energies, the photoelectrons emitted by the spacecraft dominate. These electrons are excluded from the analysis using the spacecraft potential as a threshold. The estimations of T_e were found in good agreement with the temperature computed from three-dimensional full distributions at spin resolution, for which no assumptions on the shape of the distribution function were made. The differences between sub-spin and spin resolution values of the temperature give an indication of the error associated with the sub-spin estimations. For this case, the difference is $\sim$10%, which corresponds to $\sim$3 eV given that the average electron temperature for this event is $\sim$30 eV.

Figure 4 shows the local increase in the estimated electron temperature for each detected current sheet as a function of their PVI index. The local increase was estimated by subtracting the maximum electron temperature from the median over each interval and for each spacecraft. The four estimations were averaged to yield the final value for each detected structure. It must be noted that for each detected structure, the four estimations from each spacecraft showed a profile similar to the average of the four. Most of the structures with low PVI ($1 < \mathrm{PVI} < 3$) show a small increase in the electron temperature. For comparison, the standard deviation of the electron temperature during this event is 6 eV and is marked with a dashed red line in Figure 4. Most of the structures with high PVI ($\mathrm{PVI} > 3$), however, exhibit a significantly larger increase, indicating electron heating in those structures. The observed heating corresponds to an increase up to $\sim$0.5 times the background temperature. This is shown in more detail in Table 1. For $\sim$90% of the low PVI population, the temperature increase is below 1σ. Most of the high PVI structures show a temperature increase between $1\sigma_{T_e}$ and $3\sigma_{T_e}$, with a small percentage being above 3σ. This trend becomes even more significant for the structures with very high PVI index (PVI > 5), where $\sim$80% have $\Delta T_e > 1\sigma$ and $\sim$10% are above $3\sigma_{T_e}$. Such high PVI structures have been associated with an increased probability to be sites of magnetic reconnection in numerical and recent observational studies (Servidio et al. 2011; Osman et al. 2014). We also note that significant heating is observed in a few low PVI cases.

5. CONCLUSIONS

The present work is the first statistical study of electron heating in thin current sheets in space plasma turbulence and it expands upon the results of one previous study of turbulent reconnection where electron heating was observed for a single current sheet (Retinò et al. 2007). Observations are performed in the magnetosheath downstream of the Earth's quasi-parallel shock. Current sheets have a thickness of a few proton inertial lengths and below.

The major finding of this study is that substantial heating occurs within current sheets having high PVI (>3) corresponding to regions of strong current. The increase in temperature is up to $\sim$0.5 times the background temperature and such current sheets account for $\sim$15% of the total population. High PVI current sheets in this event are often associated with high magnetic shear angles, in agreement with earlier observations (Zhdankin et al. 2012). Our observations strongly suggest that such current sheets are sites of major energy dissipation at proton scales and below. However, further studies are needed to fully address the role of high PVI current sheets and local electron heating for energy dissipation at kinetic scales, e.g., in forming the transition range in turbulent spectra observed intermittently in solar wind data, which has not yet been fully explained (Sahraoui et al. 2009, 2010).

A subset of such current sheets ($\sim$2% of the total population) correspond to very high PVI (>5) and always have very high magnetic shear angles (>90°). Such current sheets show on average stronger electron heating and therefore stronger dissipation, as found in numerical simulations (Wan et al. 2012; Karimabadi et al. 2013). Numerical simulations by Karimabadi et al. (2013) strongly suggest that the dominant heating mechanism is due to parallel electric fields associated with reconnection. Observations of reconnection at the magnetopause also indicate that stronger heating occurs at larger shear angles (Phan et al. 2013). High PVI/shear angles have been shown to be associated with ongoing reconnection (Retinò et al. 2007; Sundkvist et al. 2007; Servidio et al. 2009, 2011; Osman et al. 2014). All this indicates that the current sheets with very high PVI (>5) found in this study are likely to be reconnection sites, strongly suggesting that reconnection is a major mechanism for dissipation and electron heating in turbulence at kinetic scales. Other simulations suggest that electron heating could also be due to resonant wave-particle interactions within the current sheets, e.g., Landau damping (TenBarge & Howes 2013). Further studies are required to identify the exact heating mechanisms.

For the overwhelming majority of low PVI (<3) structures, the observed electron heating is small. Specifically, $\sim$90% of them have $\Delta T_e > 1\sigma$, see Figure 4(A). This indicate that low PVI structures are not important for energy dissipation, in agreement with earlier observations (Osman et al. 2011, 2014) and numerical simulations (Servidio et al. 2011; Wan et al. 2012; Karimabadi et al. 2013, 2014). However, low PVI current sheets should be studied in more detail to confirm their role for heating and dissipation. Among low PVI current sheets having $\Delta T_e < 1\sigma$, most of them have small magnetic shear. For such current sheets, magnetic reconnection is expected to be unfrequent (Servidio et al. 2011; Osman et al. 2014). However, such low-shear reconnection has been observed, e.g., in the solar wind (Gosling & Phan 2013), and the heating occurring therein, while small, could be still relevant given the large number of such current sheets. On the other hand, a few low PVI current sheets show $\Delta T_e > 1\sigma$. Such current sheets could be associated to other processes e.g., formation of steepening waves and shocklets as found in one case (not shown) and may contribute to heating.

Finally, our results provide an observational verification of recent kinetic simulations (Karimabadi et al. 2014) indicating that turbulence downstream of the quasi-parallel shock is comprised of volume-filling current sheets and it is an important region for turbulent dissipation at kinetic scales. Our results may also be relevant for astrophysical applications, e.g., recent studies suggest that the most efficient particle acceleration and generation of magnetic turbulence at supernova remnant shocks is found when the shock is quasi-parallel (Reynoso et al. 2013).

Sub-spin resolution electron measurements have been crucial for this study. However, such data have several limitations. Full three-dimensional particle distribution functions capable to resolve current sheets at proton scales and below are needed, e.g., to quantitatively establish how many high PVI thin current sheets are associated to reconnection and, more in general, how common reconnection is in turbulence. Such measurements will be provided by the upcoming MMS mission as well as from other future missions currently under study, e.g., *THOR*.

We thank the ESA Cluster Active Archive for providing the data for this study. The data processing of CLUSTER data at LPP is supported by CNES. We thank E. Lucek and the FGM team for the magnetic field data and A. N. Fazakerley and the PEACE team for the electron data. This work is part of the science goals of the ANR project THESOW and of the ISSI group “Kinetic turbulence and heating in the solar wind” led by F.S. and D.S. A.C.G. and F.S. acknowledge financial support from ANR/THESOW. A.C.G., A.R., F.S., A.V., D.S., and L.S. V. acknowledge financial support from ISSI. L.S.V. acknowledges support from the Italian CNR Short Term Mobility Program 2014.

REFERENCES

Balogh, A., Dunlop, M. W., Cowley, S. W. H., et al. 1997, SSRv, 79, 65
Bruno, R., & Carbone, V. 2013, LRSP, 10, 2
Chian, A. C.-L., & Muñoz, P. R. 2011, ApJL, 733, L34
Dunlop, M. W., Balogh, A., Glassmeier, K.-H., & Robert, P. 2002, JGR, 107, 1384
Escoubet, C. P., Schmidt, R., & Goldstein, M. L. 1997, SSRv, 79, 11
Gosling, J. T., & Phan, T. D. 2013, ApJL, 763, L39
Gosling, J. T. 2007, ApJL, 671, L73
Greco, A., Matthaeus, W. H., Servidio, S., Chuychai, P., & Dmitruk, P. 2009, ApJL, 691, L111
Greco, A., Chuychai, P., Matthaeus, W. H., Servidio, S., & Dmitruk, P. 2008, GeoRL, 35, 19111
Johnstone, A. D., Alsop, C., Burge, S., et al. 1997, SSRv, 79, 351
Karimabadi, H., Roytershteyn, V., Vu, H. X., et al. 2014, PhPl, 21, 062308
Karimabadi, H., Roytershteyn, V., Wan, M., et al. 2013, PhPl, 20, 012303
Khotyaintsev, Y. V., Vaivads, A., Retinò, A., et al. 2006, PhRvL, 97, 205003
Lewis, G. R., André, N., Arridge, C. S., et al. 2008, P&SS, 56, 901
Li, G. 2008, ApJL, 672, L65
Matthaeus, W. H., & Lamkin, S. L. 1986, PhFl, 29, 2513
Miao, B., Peng, B., & Li, G. 2011, AnGp, 29, 237
Nakamura, R., Baumjohann, W., Asano, Y., et al. 2006, JGR, 111, 11206
Osman, K. T., Matthaeus, W. H., Gosling, J. T., et al. 2014, PhRvL, 112, 215002
Osman, K. T., Matthaeus, W. H., Greco, A., & Servidio, S. 2011, ApJL, 727, L11
Perri, S., Goldstein, M. L., Dorelli, J. C., & Sahraoui, F. 2012, PhRvL, 109, 191101
Phan, T. D., Shay, M. A., Gosling, J. T., et al. 2013, GeoRL, 40, 4475
Retinò, A., Sundkvist, D., Vaivads, A., et al. 2007, NatPh, 3, 236
Retinò, A., Vaivads, A., André, M., et al. 2006, GeoRL, 33, 6101
Reynoso, E. M., Hughes, J. P., & Moffett, D. A. 2013, AJ, 145, 104
Sahraoui, F., Goldstein, M. L., Belmont, G., Canu, P., & Rezeau, L. 2010, PhRvL, 105, 131101
Sahraoui, F., Goldstein, M. L., Robert, P., & Khotyaintsev, Y. V. 2009, PhRvL, 102, 231102
Schwartz, S. J., Henley, E., Mitchell, J., & Krasnoselskikh, V. 2011, PhRvL, 107, 215002
Servidio, S., Greco, A., Matthaeus, W. H., Osman, K. T., & Dmitruk, P. 2011, JGR, 116, 9102
Servidio, S., Matthaeus, W. H., Shay, M. A., Cassak, P. A., & Dmitruk, P. 2009, PhRvL, 102, 115003
Sonnerup, B. U. Ö. 1979, Solar System Plasma Physics, Vol. 3 (Amsterdam: North-Holland)
Sundkvist, D., Retinò, A., Vaivads, A., & Bale, S. D. 2007, PhRvL, 99, 025004
TenBarge, J. M., & Howes, G. G. 2013, ApJL, 771, L27
Vaivads, A., Khotyaintsev, Y., André, M., et al. 2004, PhRvL, 93, 105001
Vaivads, A., Retinò, A., & André, M. 2006, SSRv, 122, 19
Varsani, A., Owen, C. J., Fazakerley, A. N., et al. 2014, AnGp, 32, 1093
Vörös, Z., Sasunov, Y. L., Semenov, V. S., et al. 2014, ApJL, 797, L10
Wan, M., Matthaeus, W. H., Karimabadi, H., et al. 2012, PhRvL, 109, 195001
Zank, G. P., le Roux, J. A., Webb, G. M., Dosch, A., & Khabarova, O. 2014, ApJ, 797, 28
Zhdankin, V., Boldyrev, S., & Mason, J. 2012, ApJL, 760, L22